Full-length article

Effects of endogenous sulfur dioxide on monocrotaline-induced pulmonary hypertension in rats[1]

Hong-fang JIN[2,5], Shu-xu DU[2,5], Xia ZHAO[2], Hong-ling WEI[2], Yan-fei WANG[2], Yin-fang LIANG[2], Chao-shu TANG[3,4,6], Jun-bao DU[2,4,6]

[2]Department of Pediatrics and [3]Institute of Cardiovascular Research, Peking University First Hospital, Beijing 100034, China; [4]Key Laboratory of Molecular Cardiovascular Diseases, Ministry of Education, Beijing 100083, China

Key words

Abstract

Aim: The present study aimed to explore the protective effect of endogenous sulfur dioxide (SO_2) in the development of monocrotaline (MCT)-induced pulmonary hypertension (PH) in rats. **Methods:** Forty Wistar rats were randomly divided into the MCT group receiving MCT treatment, the MCT+L-aspartate-β-hydroxamate (HDX) group receiving MCT plus HDX treatment, the MCT+SO_2 group receiving MCT plus SO_2 donor treatment, and the control group. Mean pulmonary artery pressure (mPAP) and structural changes in pulmonary arteries were evaluated. SO_2 content, aspartate aminotransferase activity, and gene expression were measured. Superoxide dismutase (SOD), glutathione peroxidase (GSH-Px), catalase (CAT), reduced glutathione (GSH), oxidized glutathione, and malondialdehyde (MDA) levels were assayed. **Results**: In the MCT-treated rats, mPAP and right ventricle/(left ventricle+septum) increased significantly ($P<0.01$), pulmonary vascular structural remodeling developed, and SOD, GSH-Px, CAT, GSH, and MDA levels of lung homogenates significantly increased ($P<0.01$) in association with the elevated SO_2 content, aspartate aminotransferase activity, and gene expression, compared with the control rats. In the MCT+HDX-treated rats, lung tissues and plasma SO_2 content and aspartate aminotransferase activities decreased significantly, whereas the mPAP and pulmonary vascular structural remodeling were markedly aggravated with the decreased SOD, CAT, and GSH levels of lung tissue homogenates compared with the MCT-treated rats ($P<0.01$). In contrast, with the use of a SO_2 donor, the pulmonary vascular structural remodeling was obviously lessened with elevated lung tissue SOD, GSH-Px, and MDA content, and plasma SOD, GSH-Px, and CAT levels. **Conclusion**: Endogenous SO_2 might play a protective role in the pathogenesis of MCT-induced PH and promote endogenous antioxidative capacities.

Introduction

Pulmonary hypertension (PH) is characterized by high pressure in the pulmonary artery and high pulmonary vascular resistance, ultimately inducing right ventricular failure and death with pathological changes in precapillary pulmonary arteries[1,2]. The pathophysiology of PH involves alterations in vascular reactivity, vascular structure, and interactions of the vessel wall with circulating blood elements[3,4], especially the structural remodeling of pulmonary arteries and the infiltration of perivascular inflammation. Although it has been demonstrated that endothelin, atrial natriuretic peptide, angiotensin II, serotonin, and adrenomedullin participate in the process of PH[5–8], the pathogenesis of PH is not completely understood.

Over the last 2 decades, the discovery of endogenous gas signal molecules, including nitric oxide (NO), carbon

monoxide (CO), and hydrogen sulfide (H_2S), have created a better understanding of $PH^{[9–11]}$. NO is endogenously produced by NO synthase via the metabolism of *L*-arginine and exerts potent pulmonary vasodilation and the inhibition of smooth muscle cell (SMC) proliferation, and therefore may regulate vascular remodeling[12,13]. CO, which is also endogenously produced by heme oxygenase via the metabolism of heme to biliverdin, can prevent the elevation of right ventricular systolic pressure and can partially normalize the thickened intra-acinar pulmonary arteries[14]. Endogenous H_2S can be metabolized from *L*-cysteine by cystathionine γ-lyase (CSE), a pyridoxal-5′-phosphate-dependent enzymes, in the cardiovascular system[15]. The previous study suggested that dysfunction of endogenous H_2S/CSE pathway was involved in the development of $PH^{[11,16]}$. However, the precise mechanism of PH still remains to be elucidated.

Recently, it has been proven that sulfur dioxide (SO_2) and its derivatives can relax the isolated aortic ring *in vitro* and lower blood pressure *in vivo*[17,18]. It has also been proven that sulfite is generated, at least in part, from 3′-phosphoadenosine 5′-phosphosulfate by activated neutrophils[19] and has been proposed to act as an endogenous mediator in host defense and/ or inflammation[20]. Therefore, in the present study, we employed monocrotaline (MCT), a pyrrolizidine alkaloid, to induce pulmonary artery smooth muscle hypertrophy and PH in a rat model[21,22]. We then examined the SO_2 concentration and aspartate aminotransferase (a key enzyme of endogenous SO_2 generation) activity in plasma or lung tissue homogenates of MCT-induced pulmonary-hypertensive rats. We also measured the changes of pulmonary artery pressure and pulmonary vascular structural remodeling. It has been reported that oxidative stress greatly contributes to the pathogenesis of MCT-induced $PH^{[23,24]}$, and SO_2 can cause lipid peroxidation and changes of antioxidative status in the lungs and heart of mice[25]. Therefore, we assayed the antioxidative enzymes and production of lipid peroxidation of plasma and lung tissue in MCT-treated rats to explore the possible mechanisms by which endogenous SO_2 regulates MCT-induced PH.

Materials and methods

Reagents Sodium sulfite (Na_2SO_3) and sodium bisulfite ($NaHSO_3$) were used as the SO_2 donor (mole ratio was adjusted to approximately 3:1, pH 7.4). *L*-aspartate-β-hydroxamate (HDX, an aspartate aminotransferase inhibitor), MCT, and monobromobimane (mBrB) were purchased from Sigma (St Louis, MO, USA). TRIzol, M-MuLV reverse transcriptase, dNTP, *Taq* DNA polymerase, and oligo(dT)$_{18}$ primer were obtained from Promega (Madison, WI, USA). Other chemicals and reagents were of analytical grade.

Animal preparation Animal care and experimental protocols complied with the Animal Management Rule of the Ministry of Health, China (documentation 55, 2001) and the Animal Care Committee of Peking University First Hospital, Beijing, China. Forty male Wistar rats (body weight 150±5 g) were obtained from the Experimental Animal Center, Peking University Health Science Center, Beijing, China.

The rats were randomized into the following groups: control group, MCT group, MCT+HDX group, and MCT+SO_2 group (*n*=10 for each group). The rats in the control group were administered saline water; the rats in the MCT group were injected with MCT (60 mg/kg intraperitoneally) on d 1; the rats in the MCT+HDX group were given HDX (25 mg/kg orally on d 0, 7 and 14) after injection with MCT; and the rats in the MCT+SO_2 group were subcutaneously injected with the SO_2 donor (Na_2SO_3/ $NaHSO_3$, 72.3 mg/kg) every day.

MCT (100 mg crotaline; Sigma, USA) was dissolved in 0.6 mL of 1 mol/L HCl followed by the addition of 1–2 mL distilled water. This solution was adjusted to pH 7.4 using 1 mol/L NaOH solution with 5 mL distilled water. The rats received a single subcutaneous injection of MCT solution or saline solution. The animals were housed with a 12 h light/12 h dark cycle and given water and standard rat chow ad libitum. At 3 weeks after injection, the rats were killed and the organs were harvested for the following analyses.

Measurement of hemodynamic parameters and sample preparation On d 22, the rats were weighed and anesthetized with 12% ethylcarbamate (10 mL/kg body weight) intraperitoneally. A polyethylene catheter (0.9 mm in outer diameter, PE-50, Intramedic, Sarasota, FL, USA) was introduced into the right jugular vein and passed across the tricuspid valve and right ventricle (RV) into the pulmonary artery. The catheter was filled with 0.9% NaCl containing 25 U/mL bovine heparin. The other end of the catheter was connected to a pressure transducer (PT-100, Chengdu Technology & Market Co LTD, Chengdu, China), and mean pulmonary artery pressure (mPAP) was simultaneously recorded on a physiological polygraph instrument (BL-420F New centrary, Chengdu Technology & Market Co LTD, Chengdu, China). The right lung was

rapidly isolated, snap frozen and then stored in liquid nitrogen. The heart was removed and the RV and the left ventricle (LV) plus the septum (SP) were dissected. These tissues were blotted and weighed using an electronic scale. The ratio of the wet weight of the RV to that of the LV+SP [RV/(LV+SP)] was calculated as an indicator of RV hypertrophy. Plasma was collected from the rats, centrifuged, and stored at –70 °C.

Morphometric analysis of small pulmonary arteries The left lower part of the lung tissue was removed and immersed into 10% (*w/v*) paraformaldehyde. The lung tissues were then dehydrated, embedded in paraffin, and sectioned at a thickness of 4 μm. The elastic fiber in the lung tissues was stained according to the modified Weigert's method and counterstained with Van Gieson solution. A morphological analysis was performed using a video-linked microscope digitizing board system (Leica Q550CW, Vizla, Germany). The inflammatory cells were semiquantified by the total number of the mononuclear cells around both small and medial arteries in the sections (cells/mm^2) of each section. Only vessels showing clearly defined external and internal elastic lamina were used in analysis. In this study, according to Barth's methods[26], which renders obliquely-cut arterial vessels able to be assessed accurately for medial thickness by planimetry, we defined the medial and small pulmonary arteries as those with an outer diameter ranging from 50 to 150 μm, and 15 to 50 μm, respectively, and calculated the relative medial thickness (RMT) and relative medial areas (RMA). Barth's methods consider α the angle at which a vessel is cut as an important parameter of vessel geometry. Based on α known, the shape of the obliquely cut artery is mathematically transformed to its ideal concentric circular shape.

A small part of the lung tissue was cut from the upper part of left lung lobe and quickly immersed into 3% glutaraldehyde. It was then cut into 1 mm×1 mm×1 mm pieces and post-fixed in 1% phosphate-buffered osmium tetroxide for 6 h. It was then rinsed again (overnight) and dehydrated in a graded series of ethanol. These specimens were infiltrated with propylene oxide and embedded with Epon812. These procedures were all done at room temperature. Finally, the specimens were embedded in new batches of Epon812 and polymerized at 40 °C (24 h) and 60 °C (48 h). From the selected blocks, a series of transverse or longitudinal sections were made. Semithin sections (1 μm) were stained with Azur II and methylene blue. Ultra-thin sections (60–90 nm) were made with an ultra microtome and mounted on formvar-coated copper grids (75 meshes). Then it was stained with uranyl acetate and lead citrate, and examined in detail under a transmission electron microscope (JEM-100CX; JEOL, Tokyo, Japan).

Determination of SO$_2$ content in plasma and lung tissues Samples taken from plasma and lung tissue homogenates were prepared, and the high performance liquid chromatography (HPLC) with fluorescence determination was used to determine the SO$_2$ concentration[27,28]. Briefly, 100 μL sample was mixed with 70 μL of 0.212 mol/L sodium borohydride in 0.05 mol/L Tris-HCl (pH 8.5) and incubated at room temperature for 30 min. The sample was then mixed with 10 μL of 70 mmol/L mBrB in acetonitrile, incubated for 10 min at 42 °C, and then mixed with 40 μL of 1.5 mol/L perchloric acid. The protein precipitate in the mixture was removed by centrifugation at 12 400×*g* for 10 min at 23 °C. The supernatant was immediately neutralized by adding 10 μL of 2 mol/L Tris-HCl (pH 3.0) and centrifuged at 12 400×*g* for 10 min. The neutralized supernatant was used for HPLC. The column (4.6×150 mm C18 reverse-phase column; Agilent series 1100; Agilent Technologies, Waldbronn, Karsruhe, Germany) was first equilibrated with a buffer (methanol:acetic acid: water=5.00:0.25:94.75 by volume, pH 3.4). The sample loaded onto the column was resolved by a gradient of methanol (0–5 min at 5%, 5–10 min at 35%, 10–17 min at 45%, 17–22 min at 100%, and 22–27 min at 5%) at a flow rate of 1.0 mL/min. Sulfitebimane was measured by excitation at 392 nm and emission at 479 nm.

Assay of aspartate aminotransferase activity Aspartate aminotransferase activity in plasma and lung tissue homogenates was determined by the use of a continuous assay and a biochemistry analyzer (Hitachi 7600; Tokyo, Japan). Tissue aspartate aminotransferase activity was expressed as U/g protein.

Determination of aspartate aminotransferase 1/ aspartate aminotransferase 2 mRNA in lung tissues by quantitative real-time PCR Total RNA in the lung tissue was extracted by TRIzol reagent and reverse transcribed by oligod(T)$_{18}$ primer and M-MuLV reverse transcriptase. The primers and probes used are listed in Table 1. Quantitative real-time PCR was performed on an ABI PRISM 7300 instrument (ABI USA Sales Corp, Los Angeles, CA, USA). The PCR mixture contained 5 μL of 10×PCR buffer, 5 μL cDNA template or standard DNA, 4 μL of 2.5 mmol/L each dNTP, 5 U *Taq* DNA polymerase, 1 μL 6-carboxy-X-rhodamine (ROX, Category No 12223-012; Invitrogen, Carsbad, CA, USA), 15 pmol each forward and reverse

primers, and 10 pmol *Taq* Man probe in a total volume of 50 µL. Samples and standard DNA were determined in duplicate. The PCR condition was predenaturing at 95 °C for 5 min, then 95 °C for 15 s, and 60 °C for 1 min for 40 cycles.

Measurements of lung tissue oxidants and anti-oxidative enzymes The left lung was rinsed with saline through the pulmonary artery and resected. Nine-fold volume of phosphate-buffered saline (PBS) was added and then grinded gently at 4 °C. Superoxide dismutase (SOD), glutathione peroxidase (GSH-Px), catalase (CAT), reduced glutathione (GSH), oxidized glutathione (GSSG), and malondialdehyde (MDA) of the lung tissue homogenates and plasma were determined by colorimetric method using corresponding kits (Nanjing Jiancheng Biology, Nanjing, China).

Statistics The results are expressed as mean±SD. All data were analyzed with SPSS 11.5 (SPSS, Chicago, IL, USA). ANOVA, followed by *post-hoc* analysis, (Newman–Keuls test) was used to compare differences among groups. *P*-values less than 0.05 were considered statistically significant.

Results

Rat model of PH A single intraperitoneal injection of MCT resulted in a significant increase in mPAP of the rats in the MCT group after 3 weeks of the experiment compared with the control group ($P<0.01$). This was paralleled by right ventricular hypertrophy with an increased RV/(LV+SP) weight ratio (an index of RV hypertrophy) at 3 weeks ($P<0.01$). Moreover, the rats of the MCT group had significantly lower body weight after 3

Table 2. Comparison of mPAP, RV/(LV+SP) ratio and BW among 4 groups of rats. *n*=10. Mean±SD. $^{c}P<0.01$ *vs* control group. $^{f}P<0.01$ *vs* MCT group.

Groups	mPAP (mmHg)	RV/(LV+SP) ratio	BW (g)
MCT group	38.18±6.15^{c}	0.57±0.06^{c}	236±17^{c}
MCT+HDX group	47.61±7.26^{cf}	0.65±0.06^{cf}	233±21^{c}
MCT+SO$_2$ group	38.91±8.55^{c}	0.55±0.05^{c}	227±27^{c}
Control group	15.75±2.41	0.31±0.03	271±24

mPAP, mean pulmonary artery pressure. RV/(LV+SP), right ventricular weight/left ventricular plus septum weight. BW, body weight. MCT, monocrotaline. SO$_2$, sulfur dioxide. HDX, *L*-aspartate-β-hydroxamate.

weeks of the experiment ($P<0.01$, Table 2).

Morphometric analysis of pulmonary arteries in MCT-induced pulmonary-hypertensive rats A histological examination of the lungs at 3 weeks after MCT injection revealed interstitial thickening and prominent media hypertrophy of muscular pulmonary arteries and arterioles. Lumens of arteries were narrowed, even occluded, and the normal structure of artery wall was remodeled. Compared with the control rats, the total number of monocular cells around the arteries in the sections was significantly increased in the rats of the MCT group (54.35±18.75 cells/mm^2 *vs* 14.25±5.25 cells/mm^2 ($P<0.01$, Figure 1). Compared with the rats in the control group, RMT and RMA, defined as parameters of pulmonary vascular structural remodeling, were increased significantly in the medial and small pulmonary arteries (all $P<0.01$), together with the development of PH in the rats of the MCT group (Table 3, Figure 2). Furthermore, the endothelial cells (EC) were swollen and hypertrophic,

Table 1. Primers and TaqMan probes used in quantitative real time RT-PCR for the measurement of aspartate aminotransferase 1, aspartate aminotransferase 2 and β-actin cDNAs in rat.

cDNA	Oligonucleotide	Sequence	Product size (bp)
Aspartate amino transferase 1	Forward primer	5'-CCAGGGAGCTCGGATCGT-3'	79
	Reverse primer	5'-GCCATTGTCTTCACGTTTCCTT-3'	
	TaqMan probe	5'-CCACCACCCTCTCCAACCCTGA-3'	
Aspartae amino transferase 2	Forward primer	5'-GAGGGTCGGAGCCAGCTT-3'	82
	Reverse primer	5'-GTTTCCCCAGGATGGTTTGG-3'	
	TaqMan probe	5'-TTTAAGTTCAGCCGAGATGTCTTTC-3'	
β-actin	Forward primer	5'-ACCCGCGAGTACAACCTTCTT-3'	80
	Reverse primer	5'-TATCGTCATCCATGGCGAACT-3'	
	TaqMan probe	5'-CCTCCGTCGCCGGTCCACAC-3'	

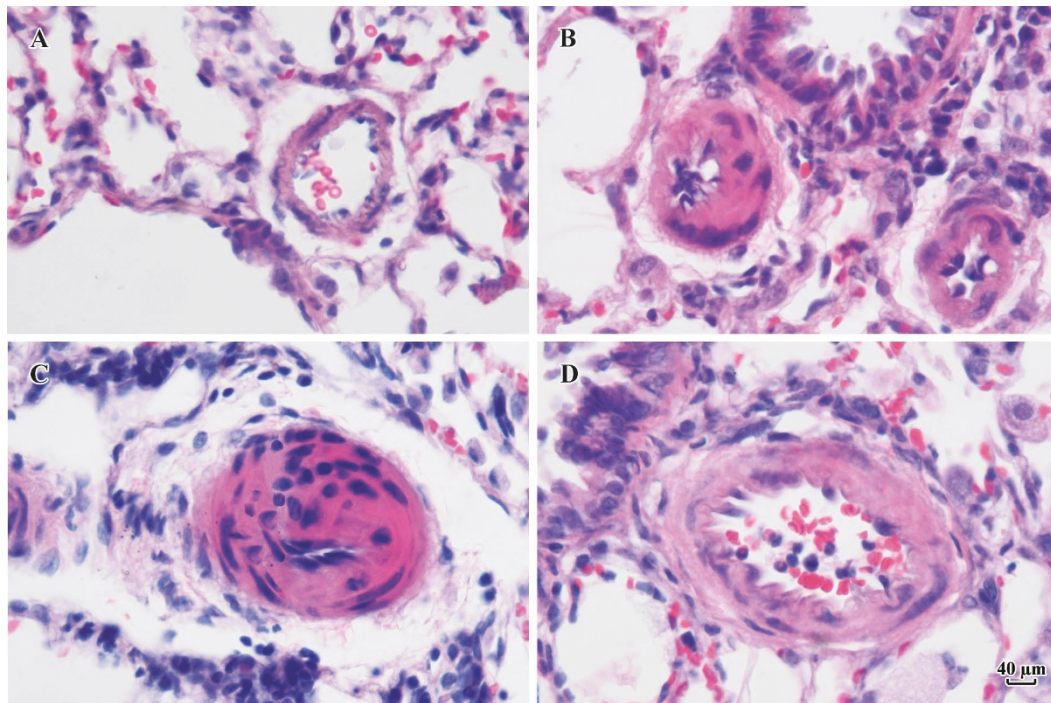TaqMan probe labeled with FAM at the 5′ end and TAMRA at the 3′ end.

Figure 1. Microstructural changes in rat lung. (A) control group: the normal lung arteriole wall was thin, and endothelial cells were flat and continuous. Cells distributed well, and the size and thickness were consistent. (B) MCT group: the interstitial thickening and prominent media hypertrophy of muscular pulmonary arteries and arterioles were shown. Lumens of arteries were narrowed, even occluded, normal structure of arteriolar wall disappeared, and inflammatory cells infiltrated around the arteriole. Compared with control group, the total number of inflammatory cells (neutrophils and lymphocytes) in sections was significantly increased in MCT rats. (C) MCT+HDX group: the pathological changes were much aggravated. Compared with those of MCT group, less inflammatory cells infiltrated at both perivascular and peribronchial areas in MCT+HDX group. (D) MCT+SO$_2$ group: the interstitial thickening and prominent media hypertrophy of muscular pulmonary arteries and arterioles were attenuated significantly, though the infiltration of inflammatory cells was increased compared with MCT group. (HE staining, ×400).

the internal elastic lamina appeared irregular, and rough endoplasmic reticulum and free ribosomes increased in the cytoplasm of SMC in the rats of the MCT group (Figure 3).

Alteration of the SO$_2$/aspartate aminotransferase pathway in MCT-induced pulmonary hypertensive rats The aspartate aminotransferase activity and

Table 3. RMT and RMA changes of medium and small pulmonary arteries of 4 groups of rats. *n*=10. Mean±SD. $^c P<0.01$ *vs* control group. $^e P<0.05$ *vs* MCT group.

Groups	Small pulmonary artery		Medium pulmonary artery	
	RMT (%)	RMA (%)	RMT (%)	RMA (%)
MCT group	9.39±2.34^c	17.84±4.16^c	15.07±4.72^c	29.35±3.84^c
MCT+HDX group	11.99±1.94^{ce}	20.54±8.59^{ce}	17.59±5.04^{ce}	31.86±4.13^c
MCT+SO$_2$ group	6.53±2.10^e	12.59±3.91^e	13.65±4.11^e	25.29±6.96^e
Control group	5.29±2.21	10.26±4.15	11.19±2.58	21.85±4.56

MCT, monocrotaline. SO$_2$, sulfur dioxide. HDX, *L*-aspartate-β-hydroxamate. RMT, relative medium thickness. RMA, relative media area.

SO$_2$ concentration in the lung tissues was increased significantly of the rats of the MCT group (all *P*<0.01). The aspartate aminotransferase activity in plasma was also increased obviously (*P*<0.01, Table 4). Compared with the control group, aspartate aminotransferase 1 mRNA levels in the lung tissues of the rats in the MCT group were increased obviously (*P*<0.01). Meanwhile, aspartate aminotransferase 2 mRNA levels in the lung tissues and pulmonary arteries of the rats in the MCT group were higher than that of the control group (all *P*<0.01, Table 5).

Effects of endogenous SO$_2$ on MCT-induced PH and pulmonary artery structural remodeling The aspartate aminotransferase activity and SO$_2$ concentration in the lung tissues and plasma of the rats in the MCT+HDX group decreased markedly (all *P*<0.01, Table 4). However, the aspartate aminotransferase 2 mRNA in the lung tissues and pulmonary arteries of the rats in the MCT+HDX group was further increased, respectively (all *P*<0.01; Table 5). Meanwhile, the aspartate aminotransferase 1 mRNA in the lung tissues of the rats in the MCT+HDX group also
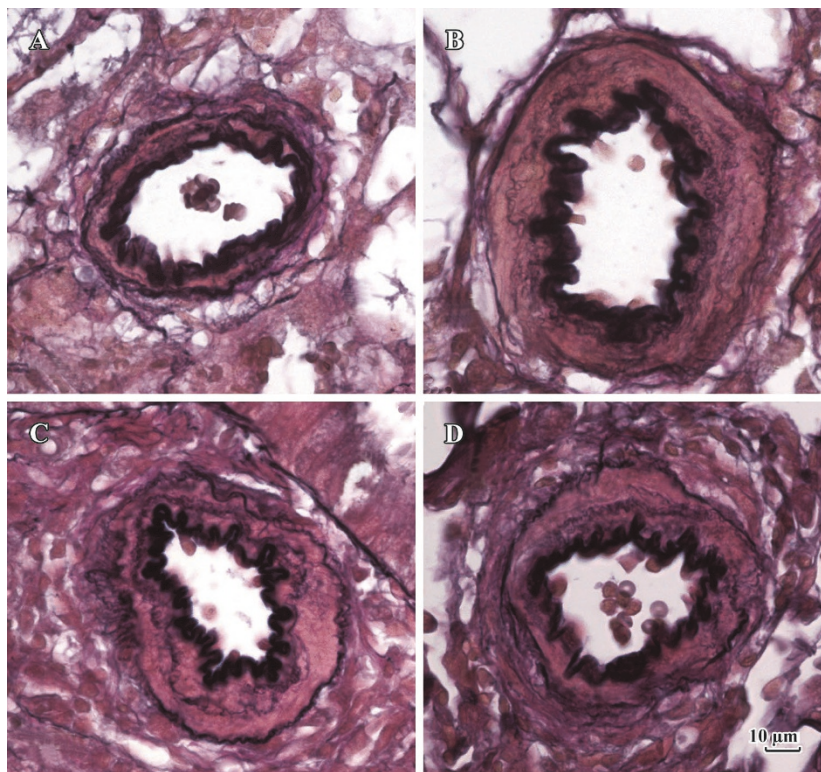
Figure 2. Elastin fiber staining of small pulmonary arteries under optical microscope. (A) control group: the wall of small pulmonary artery exhibited a normal structure. (B) MCT group: the wall of small pulmonary artery was thick compared with that of control rat. (C) MCT+HDX group: the wall of small pulmonary artery was thicker than that of MCT-treated rat. (D) MCT+SO$_2$ group: the wall of small pulmonary artery was thinner than that of MCT-treated rat. (×400).
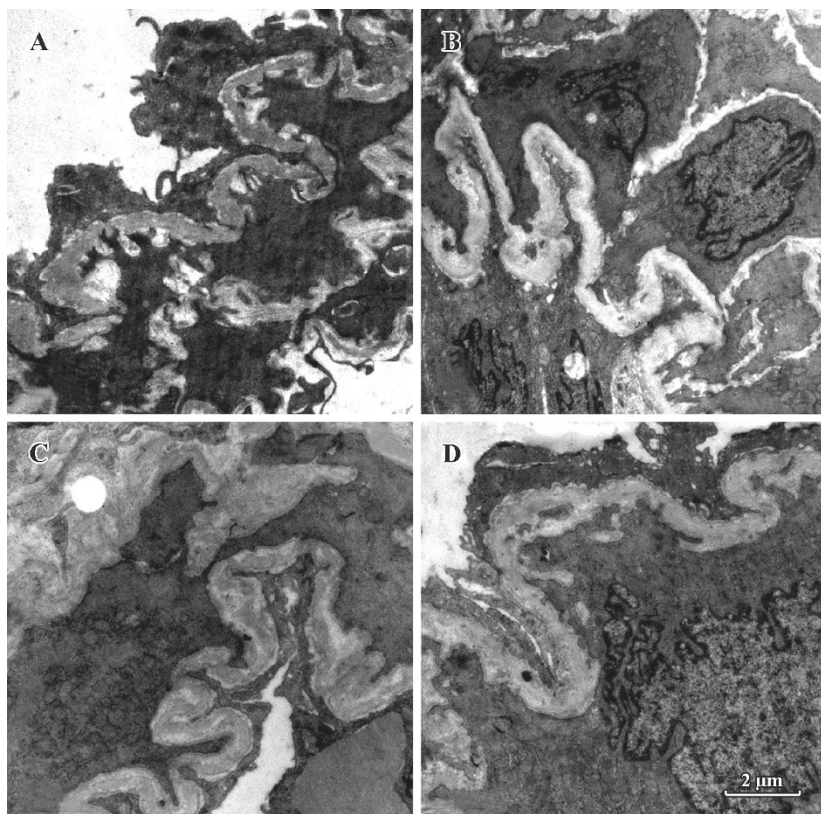

Figure 3. Ultra-structural changes of rat lung tissues. (A) control group: the normal vascular endothelial cells (VECs) were flat and thin, inner elastic layer thickness was even, and smooth muscle cells were in fusiform shape. Structures of actin filament, dense body and dense patch were clear. (B) MCT group: the VECs were swollen and degenerated lightly, small vacuole could be seen. The inner elastic layers were rarefaction and the thickness was not even. The smooth muscle cells were hypertrophic, and cell organs were abundant. (C) MCT+HDX group: the shape of arteriole endothelial cells was augmented to collumn shape and degenerated slightly. The inner elastic layers were much puff, smooth muscle cells were hypertrophic, and cell organs, such as chondriosome and rough endoplasmic reticulum, were abundant. (D) MCT+SO$_2$ group: the VECs proliferation and lumen stenosis still could be found, though they were flat and thin. The inner elastic layer was comparatively even. SMC also was in fusiform shape, and structure of dense body and dense patch was clear. (×12 000).

Table 4. SO$_2$/aspartate aminotransferase pathway in monocrotaline-induced PH rats. *n*=10. Mean±SD. [b]*P*<0.05, [c]*P*<0.01 *vs* control group. [e]*P*<0.05, [f]*P*<0.01 *vs* MCT group.

Groups	Aspartate aminotransferase activity		SO$_2$ content	
	Plasma (IU/L)	Lung tissue (IU/g protein)	Plasma (µg/mL)	Lung tissue (µmol/g protein)
MCT group	134.02±18.51[c]	64.42±2.80[c]	2.31±0.51	4.77±0.43[b]
MCT+HDX group	93.51±7.43[cf]	34.81±5.92[bf]	1.74±0.31[e]	2.55±0.54[bf]
MCT+SO$_2$ group	125.33±14.62[c]	50.34±4.52	4.69±1.74[cf]	9.08±1.17[cf]
Control group	80.81±8.25	53.73±4.92	1.88±0.33	3.92±0.46

MCT, monocrotaline. SO$_2$, sulfur dioxide. HDX, *L*-aspartate-β-hydroxamate.

increased obviously (*P*<0.05). The mPAP and RV/(LV+SP) of the rats in the MCT+HDX group were higher than those of the MCT group (all *P*<0.01, Table 2). Compared with the MCT group, the RMT and RMA of small pulmonary arteries in the rats of the MCT+HDX group were further increased by 27.7% and 15.1%, respectively (all *P*<0.05, Table 3, Figure 2). Meanwhile, the RMT and RMA of the medium pulmonary arteries were also increased by 16.7% and 8.5%, respectively (all *P*<0.05). In the rats of the MCT+HDX group, lung interstitial edema was aggravated, more inflammatory cells infiltrated (78.55±23.75 cells/mm^2), and most pulmonary alveoli were disorganized. The hyperplasia and shedding of type II alveolar epithelial cells were aggravated. Arteriolar EC were augmented to column shape and degenerated slightly. Lumens were obliterated, and the inner elastic layers of small pulmonary artery of the rats in the MCT+HDX group were much puff compared with that of the rats in the MCT group. SMC hypertrophy was significant, and cell organs, such as chondriosome and rough endoplasmic reticulum were more abundant as compared with the MCT group (Figure 3).

Effects of SO$_2$ donor on MCT-induced pulmonary artery structural remodeling The SO$_2$ content in the lung tissues and plasma in the rats of the MCT+SO$_2$ group were higher than that of the MCT group (all *P*<0.01; Table 4). Compared with the MCT group, the RMT and RMA of the pulmonary arteries in the rats of the MCT+SO$_2$ group decreased by 30.4% and 29.4% for small pulmonary arteries and by 9.4% and 13.8% for median pulmonary arteries, respectively (all *P*<0.05). However, the infiltration of inflammatory cells (93.75±24.68 cells/mm^2) increased obviously compared with those of the MCT group (*P*<0.05, Table 3, Figure 2).

Influence of SO$_2$ on the oxidative and antioxidative balance in MCT-induced pulmonary-hypertensive rats Compared with the control group, the activities of antioxidative enzymes, including SOD, GSH-Px and CAT, in the lung tissues of the rats in the MCT group increased significantly (all *P*<0.01), and GSH, an important antioxidant, also increased obviously (*P*<0.01). Meanwhile, oxidative production, including GSSG and MDA, in the lung tissues of the rats in the MCT group also increased markedly (*P*<0.01). Compared with the MCT group, SOD and CAT enzymatic activity and GSH content in the lung tissues in the rats of the MCT+HDX group decreased by 14.95%, 18.22%, and 15.06%, respectively (all *P*<0.05, Table 6). In the rats of MCT+SO$_2$ group, SOD and GSH-Px enzymatic activity and MDA content in the lung tissues were increased by 20.6%, 13.05%, and 13.1% compared with MCT group respectively (all *P*<0.01, Table 6). Meanwhile, SOD, GSH-Px, and CAT enzymatic activity in the plasma of the rats in the MCT+SO$_2$ group also increased obviously (*P*<0.05, Table 7).

Discussion

In the present study, we successfully established a rat model of MCT-induced PH and pulmonary vascular

Table 5. Glutamate oxaloacetate transaminase mRNA expression in MCT-induced PH rats. *n*=10. Mean±SD. [c]*P*<0.01 *vs* control group. [f]*P*<0.01 *vs* MCT group.

Groups	Lung tissues		Pulmonary artery	
	Aspartate aminotransferase 1 mRNA/β-actin mRNA	Aspartate aminotransferase 2 mRNA/β-actin mRNA	Aspartate aminotransferase 1 mRNA/β-actin mRNA	Aspartate aminotransferase 2 mRNA/β-actin mRNA
MCT group	0.16±0.02[c]	0.73±0.09[c]	0.55±0.08	0.59±0.06[c]
MCT+HDX group	0.34±0.05[cf]	2.37±0.13[cf]	0.58±0.09	1.25±0.16[cf]
MCT+SO$_2$ group	0.45±0.10[cf]	2.73±0.31[cf]	0.59±0.02	1.53±0.24[cf]
Control group	0.08±0.01	0.14±0.03	0.51±0.03	0.29±0.07

MCT, monocrotaline. SO$_2$, sulfur dioxide. HDX, L-aspartate-β-hydroxamate.

Table 6. Effects of SO_2 on the oxidative stress in the lung tissues in MCT-induced PH rats. n=10. Mean±SD. [c]$P<0.01$ *vs* control group. [e]$P<0.05$, [f]$P<0.01$ *vs* MCT group.

Groups	SOD (U/mg lung)	GSH-Px (U/mg lung)	CAT (U/mg lung)	GSH (μmol/g lung)	GSSG (μmol/g lung)	GSH/GSSG	MDA (μmol/g lung)
MCT group	118.61±8.64[c]	41.75±4.73[c]	41.27±3.95[c]	63.36±5.30[c]	35.92±4.81[c]	1.77±0.13[c]	5.34±0.31[c]
MCT+HDX group	100.88±17.97[ce]	40.35±11.63[c]	33.75±9.14[cf]	53.82±1.83[cf]	33.33±5.46	1.58±0.32[ce]	5.68±0.70[c]
MCT+SO_2 group	143.05±18.48[cf]	47.20±7.54[cf]	38.36±6.15[c]	59.10±5.95[c]	32.59±3.92	1.83±0.18[c]	6.04±0.49[cf]
Control group	82.12±4.69	27.04±4.11	22.14±3.51	41.77±6.61	34.98±3.75	1.19±0.15	4.48±0.55

MCT, monocrotaline. SO_2, sulfur dioxide. HDX, *L*-aspartate-β-hydroxamate. SOD, superoxide dismutase. GSH-Px, glutathione peroxidase. CAT, catalase. GSH, reduced glutathione. GSSG, oxidized glutathione. MDA, malondialdehyde.

Table 7. Effects of SO_2 on the oxidants and antioxidants in the plasma of MCT-induced PH rats. n=10. Mean±SD. [e]$P<0.05$ *vs* MCT group.

Groups	SOD (U/mL)	GSH-Px (U/mL)	CAT (U/mL)	GSSG (μmol/L)	MDA (μmol/L)
MCT group	68.53±7.46	74.67±11.35	24.1±5.17	41.73±15.58	6.19±1.85
MCT+HDX group	75.06±9.19	64.62±24.92	23.51±5.48	49.02±12.56	6.93±1.93
MCT+SO_2 group	79.19±7.04[e]	93.67±17.33[e]	31.04±10.41[e]	43.39±11.96	5.89±1.63
Control group	74.80±10.21	74.85±20.86	28.69±5.30	37.28±16.83	7.59±1.27

MCT, monocrotaline. SO_2, sulfur dioxide. HDX, *L*-aspartate-β-hydroxamate. SOD, superoxide dismutase. GSH-Px, glutathione peroxidase. CAT, catalase. GSSG, oxidized glutathione. MDA, malondialdehyde.

structural remodeling. On the basis of the rat model of MCT-induced PH, we explored the role of endogenous SO_2 in the pathogenesis of MCT-induced PH. SO_2 is best known as a common air pollutant that has resulted from increased industrial activity over the past several decades. Less recognized, however, is the fact that SO_2 is also a biological gas endogenously generated from sulfur-containing amino acids in a series of reactions catalyzed by aspartate aminotransferase[29,30].

We found that the endogenous SO_2/aspartate aminotransferase pathway was upregulated significantly in the rats of the MCT groups, exhibiting an increase in endogenous SO_2 content in the lung tissues and enhancement of aspartate aminotransferase enzymatic activity in plasma and lung tissues. Moreover, we determined the change of the aspartate aminotransferase mRNA level in the lung tissues and pulmonary arteries in the rats of the MCT group. Aspartate aminotransferase has two isoenzymes named for their intracellular location: aspartate aminotransferase 1 is located in the cell cytoplasm, and aspartate aminotransferase 2 is located in the cell mitochondria. Our data showed that expression of aspartate aminotransferase 1 mRNA in the lung tissues and that of aspartate aminotransferase 2 mRNA in the lung tissues and pulmonary arteries of the rats in the MCT group were increased markedly.

To further determine the significance of the SO_2/aspartate aminotransferase pathway during the development of PH in MCT-treated rats, HDX, an inhibitor of aspartate aminotransferase, was administered and significantly inhibited the activity of aspartate aminotransferase and the production of endogenous SO_2. At the same time, mPAP and RV/(LV+SP) were further increased, and the microstructure and ultrastructure of muscular pulmonary arteries worsened, which suggested that the inhibition of endogenous SO_2 can augment PH, and promote right ventricular hypertrophy and pulmonary vascular structural remodeling in MCT-treated rats. Na_2SO_3/$NaHSO_3$, a donor of exogenous SO_2, was supplied for 3 weeks and was found to significantly increase the lung tissue SO_2 content. Simultaneously, Na_2SO_3/$NaHSO_3$ alleviated small and median pulmonary artery structural remodeling. All these data implied that the upregulation of the endogenous SO_2/aspartate aminotransferase pathway might play a protective role in the process of MCT-induced PH.

However, the underlying mechanism responsible for the protective role of the endogenous SO_2/aspartate aminotransferase pathway in the development of PH is not clear. Studies have suggested that increased oxidative stress, such as the enhanced production of superoxide anions and other reactive oxygen species, might contribute to the pathogenesis and/or development of PH[31,32]. It

has also been reported that oxidative stress may in part contribute to the pathogenesis of PH in a MCT model[33,34]. The antioxidative defense is largely provided by several enzymes such as SOD, GSH-Px, and CAT[35–37]. Meng and coworkers[25] indicated that low doses of SO_2 (22 and 56 mg/m^3) caused significant increases in SOD, GSH-Px, and CAT activities in the lungs.

In the present study, the activities of those antioxidative enzymes, including SOD, GSH-Px, and CAT in the lung tissues of the MCT-treated rats increased significantly compared with the control group. Also, GSH/GSSG, which is believed to be a major element in the detoxification of SO_2[38], and MDA, lipid peroxidation production, increased markedly in the lung tissues of the rats in the MCT group. These results are in accordance with those previously reported[31,32].

Interestingly, when the endogenous SO_2 was inhibited by HDX, the antioxidative enzyme (SOD and CAT) activities and GSH levels in the lung tissues decreased significantly compared with the MCT group, suggesting that endogenous SO_2 could increase the antioxidative ability in MCT-treated rats. To further understand the effect of SO_2 on MCT-induced oxidative stress, we observed the changes in oxidative stress and the antioxidative status in the rats of the MCT+SO_2 group. Compared with the MCT group, the activities of those antioxidative enzymes, including SOD and GSH-Px in the lung tissues were increased significantly. Moreover, GSH-Px and CAT activities in the plasma also increased obviously in the rats of the MCT+SO_2 group. These results imply that the SO_2 can, at least partly, increase the antioxidative capacity of rats.

Additionally, the inflammatory cell infiltration around the pulmonary arteries in the rats of the MCT group were worsened following administration of HDX, suggesting that the inhibition of perivascular inflammation might be involved in the regulatory effect of endogenous SO_2. However, Na_2SO_3/$NaHSO_3$ was found to aggravate inflammatory cell infiltration around the pulmonary arteries in the rats of the MCT group. The mechanisms by which the supplement of exogenous SO_2 produced such a result is unclear. A previous study showed that SO_2 inhalation (5 ppm) could increase the levels of interleukin-6 and TNF-α in lungs and sera, and cause an inflammatory reaction[39]. All these findings imply that the effect of SO_2 on perivascular inflammation might depend on the different concentrations of SO_2 in tissues. Further studies on the role of endogenous or exogenous SO_2 in the regulation of inflammation are needed.

Previous studies on this gas molecule have focused on the toxicity and oxidative damage of exogenous SO_2 inhalation[25,40–42]. In the present study, we first explored the pathophysiological significance of endogenous SO_2 in MCT-induced PH. Based on our studies, it is suggested that endogenous SO_2 might play a pathophysiological and protective role, at least partially, in the process of MCT-induced PH.

Author contribution

Hong-fang JIN, Shu-xu DU, Chao-shu TANG, and Jun-bao DU designed research, Shu-xu DU, Xia ZHAO, Hong-ling WEI, and Yan-fei WANG performed research, Hong-fang JIN, Yan-fei WANG, and Yin-fang LIANG contributed new analytical tools and reagents; Hong-fang JIN, Shu-xu DU, Chao-shu TANG, and Jun-bao DU analyzed data; Hong-fang JIN, Shu-xu DU, Chao-shu TANG, and Jun-bao DU wrote the paper.

References

1　McLaughlin VV, McGoon MD. Primary pulmonary hypertension. Circulation 2006; 114: 1417–31.

2　Hoeper MM, Rubin LJ. Update in pulmonary hypertension 2005. Am J Respir Crit Care Med 2006; 173: 499–505.

3　Granton JT, Rabinovitch M. Pulmonary arterial hypertension in congenital heart disease. Cardiol Clin 2002; 20: 441–57.

4　Tuder RM, Groves B, Badesch DB, Voelkel NF. Exuberant endothelial cell growth and elements of inflammation are present in plexiform lesions of pulmonary hypertension. Am J Pathol 1994; 144: 275 –85.

5　Wu LY, Wang R. Carbon monoxide: endogenous production, physiological functions, and pharmacological applications. Pharmacol Rev 2005; 57: 585–630.

6　Yanagisawa M, Kurihara H, Kimura S, Tomobe Y, Kobayashi M, Mitsui Y, *et al*. A novel potent vasoconstrictor peptide produced by vascular endothelial cells. Nature 1988; 332: 411–5.

7　Shimokawa H, Tomoike H, Nabeyama S, Yamamoto H, Araki H, Nakamura M, *et al*. Coronary artery spasm induced in atherosclerotic miniature swine. Science 1983; 221: 560–2.

8　Vroomen M, Takahashi Y, Gournay V, Roman C, Rudolph AM, Heymann MA. Adrenomedulin increases pulmonary blood flow in fetal sheep. Pediatr Res 1997; 41: 493–7.

9　Du JB, Jia JF, Li WZ, Zhao B, Zeng HP. Nitric oxide impacts endothelin-1 gene expression in intrapulmonary arteries of chronically hypoxic rats. Angiology 1999; 50: 479–85.

10　Shi Y, Du JB, Gong LM, Zeng CM, Tang XY, Tang CS. The regulating effect of heme oxygenase/carbon monoxide on hypoxic pulmonary vascular structural remodeling. Biochem Biophys Res Commun 2003; 306: 523–9.

11　Li XH, Du JB, Shi L, Li J, Tang XY, Qi JG, *et al*. Down-regulation of endogenous hydrogen sulfide pathway in pulmonary hypertension and pulmonary vascular structural remodeling induced by high

pulmonary blood flow in rats. Circ J 2005; 69: 1418–24.

12 Ignarro LJ. Biological actions and properties of endothelium-derived nitric oxide formed and released from artery and vein. Circ Res 1989; 65: 1–2.

13 Garg UC, Hassid A. Nitric oxide-generating vasodilators and 8-bromo-cyclic guanosine monophosphate inhibit mitogenesis and proliferation of cultured rat vascular smooth cells. J Clin Invest 1989; 83: 1774 –7.

14 Zhen G, Zhang Z, Xu Y. The role of endogenous carbon monoxide in the hypoxic vascular remodeling of rat model of hypoxic pulmonary hypertension. J Huazhong Univ Sci Tech Med Sci 2003; 23: 356–68.

15 Tang CS, Li XH, Du JB. Hydrogen sulfide as a new endogenous gaseous transmitter in the cardiovascular system. Curr Vasc Pharmacol 2006; 4: 17–22.

16 Zhang CY, Du JB, Bu DF, Yan H, Tang XY, Tang CS. The regulatory effect of hydrogen sulfide on hypoxic pulmonary hypertension in rats. Biochem Biophys Res Commun 2003; 302: 810–6.

17 Meng ZQ, Zhang H. The vasodilator effect and its mechanism of sulfur dioxide-derivatives on isolated aortic rings of rats. Inhal Toxicol 2007; 19: 979–86.

18 Meng ZQ, Geng HF, Bai JL, Yan G. Blood pressure of rats lowered by sulfur dioxide and its derivatives. Inhal Toxicol 2003; 15: 951–9.

19 Mitsuhashi H, Ota F, Ikeuchi K, Kaneko Y, Kuroiwa T, Ueki K, *et al*. Sulfite is generated from PAPS by activated neutrophils. Tohoku J Exp Med 2002; 198: 125–32.

20 Shigehara T, Mitsuhashi H, Ota F, Kuroiwa T, Kaneko Y, Ueki K, *et al*. Sulfite induces adherence of polymorphonuclear neutrophils to immobilized fibrinogen through activation of Mac-1 beta2-integrin (CD11b/CD18). Life Sci 2002; 70: 2225–32.

21 Huxtable RJ. Activation and pulmonary toxicity of pyrrolizidine alkaloids. Pharmacol Ther 1990; 47: 371–89.

22 Rosenberg HC, Rabinovitch M. Endothelial injury and vascular reactivity in monocrotaline pulmonary hypertension. Am J Physiol 1988; 255: H1484–91.

23 Aziz SM, Toborek M, Hennig B, Endean E, Lipke DW. Polyamine regulatory processes and oxidative stress in monocrotaline-treated pulmonary artery endothelial cells. Cell Biol Int 1997; 21: 801–12.

24 Kamezaki F, Tasaki H, Yamashita K, Tsutsui M, Koide S, Nakata S, *et al*. Gene transfer of extracellular superoxide dismutase ameliorates pulmonary hypertension in rats. Am J Respir Crit Care Med 2008; 177: 219–26.

25 Meng Z, Qin G, Zhang B, Geng H, Bai Q, Bai W, *et al*. Oxidative damage of sulfur dioxide inhalation on lungs and hearts of mice. Environ Res 2003; 93: 285–92.

26 Barth PJ, Kimpel CH, Roy S, Wagner U. An improved mathematical approach for the assessment of the medial thickness of pulmonary arteries. Pathol Res Pract 1993; 189: 567–76.

27 Mitsuhashi H, Ikeuchi H, Yamashita S, Kuroiwa T, Kaneko Y, Hiromura K, *et al*. Increased levels of serum sulfite in patients with acute pneumonia. Shock 2004; 21: 99–102.

28 Ji AJ, Savon SR, Jacobsen DW. Determination of total serum sulfite by HPLC with fluorescence detection. Clin Chem 1995; 41: 897–903.

29 Stipanuk MH. Metabolism of sulfur containing amino acids. Annu Rev Nutr 1986; 6: 179–209.

30 Griffith OW. Cysteinesulfinate metabolism altered partitioning between transamination and decarboxylation following administration of beta-methylene aspartate. J Biol Chem 1983; 258: 1591–8.

31 Hironaka E, Hongo M, Sakai A, Mawatari E, Terasawa F, Okumura N, *et al*. Serotonin receptor antagonist inhibits monocrotaline-induced pulmonary hypertension and prolongs survival in rats. Cardiovasc Res 2003; 60: 692–9.

32 Versluis JP, Heslinga JW, Sipkema P, Westerhof N. Contractile reserve but not tension is reduced in monocrotaline-induced right ventricular hypertrophy. Am J Physiol Heart Circ Physiol 2004; 286: H979–87.

33 Ecarnot-Laubriet A, Rochette L, Vergely C, Sicard P, Teyssier JR. The activation pattern of the antioxidant enzymes in the right ventricle of rat in response to pressure overload is of heart failure type. Heart Dis 2003; 5: 308–12.

34 Farahmand F, Hill MF, Singal PK. Antioxidant and oxidative stress changes in experimental cor pulmonale. Mol Cell Biochem 2004; 260: 21–9.

35 Ceballos-Picot I, Nicole A, Clément M, Bourre JM, Sinet PM. Age-related changes in antioxidant enzymes and lipid peroxidation in brains of control and transgenic mice overexpressing copper-zinc superoxide dismutase. Mutat Res 1992; 275: 281–93.

36 Gupta A, Hasan M, Chander R, Kapoor NK. Age-related elevation of lipid peroxidation products: diminution of superoxide dismutase activity in the central nervous system of rats. Gerontology 1991; 37: 305–9.

37 Singh R, Pathak DN. Lipid peroxidation and glutathione peroxidase, glutathione reductase, superoxide dismutase, catalase, and glucose-6-phosphate dehydrogenase activities in $FeCl_3$-induced epileptogenic foci in the rat brain. Epilepsia 1990; 31: 15–26.

38 Yargicoglu P, Sahin E, Gümüşlü S, Ağar A. The effect of sulfur dioxide inhalation on active avoidance learning, antioxidant status and lipid peroxidation during aging. Neurotoxicol Teratol 2007; 29: 211–8.

39 Meng Z, Liu Y, Wu D. Effect of sulfur dioxide inhalation on cytokine levels in lungs and serum of mice. Inhal Toxicol 2005; 17: 303–7.

40 Meng Z. Oxidative damage of sulfur dioxide on various organs of mice: sulfur dioxide is a systemic oxidative damage agent. Inhal Toxicol 2003; 15: 181–95.

41 Meng Z, Bai W. Oxidation damage of sulfur dioxide on testicles of mice. Environ Res 2004; 96: 298–304.

42 Xie J, Fan R, Meng Z. Protein oxidation and DNA-protein crosslink induced by sulfur dioxide in lungs, livers, and hearts from mice. Inhal Toxicol 2007; 19: 759–65.